Utilizing Environmentally Friendly Synthetic Nanomaterials to eliminate Toludine Blue from Water

Khandelwal Vishnu Kumar[1*], Bansal Nidhi[1] and Agrawal Neetu[2]
1. Department of Chemistry, JECRC University, Jaipur, INDIA
2. Department of Chemistry, Agrawal P.G. College, Jaipur, INDIA
*vishnusmec1974@gmail.com

Abstract

Green synthesis, an eco-friendly and sustainable approach, is becoming popular for nanoparticle production. This method minimizes the use of hazardous chemicals, making it a desirable alternative for various applications. The current study focuses on synthesizing green TiO_2 NPs using Kigelia africana leaf extracts (sausage tree) and evaluating their performance in photo-catalytic treatment of textile wastewater post-secondary treatment. The TiO_2 NPs using Kigelia africana leaf extracts resulted in nanoparticles characterized by several advanced techniques, confirming their morphology, structure and composition. The synthesized TiO_2 NPs were tested for their efficiency in treating textile effluent, specifically targeting the removal of organic dyes.

SEM images revealed the morphology and size of the TiO_2 NPs. The nanoparticles were confirmed to be spherical in shape. EDX analysis provided the elemental composition of green synthesized TiO_2 NPs. Presence of titanium and oxygen elements was confirmed, validating the synthesis process. XRD patterns confirmed the crystalline structure of the TiO_2 NPs.

The nanoparticles exhibited the anatase phase known for its superior photo-catalytic properties. FT-IR spectra identified the functional groups involved in the synthesis. The presence of characteristic TiO_2 peaks was observed, indicating successful formation of TiO_2 NPs. DLS measurements provided information on the particle size distribution. The synthesized nanoparticles had a narrow size distribution, confirming their uniformity. TEM images further confirmed the spherical shape and size of the TiO_2 NPs. High-resolution images showed well-defined and uniformly distributed nanoparticles. The photo-catalytic treatment achieved a 98.69% removal of Toludine Blue (TB) dye within 65 minutes. This high efficiency demonstrates the potential of green-synthesized TiO_2 NPs in treating organic dyes in textile wastewater.

Keywords: Toludine blue, Nanoparticles, Photocatalytic, Morphology, Electro-dialysis.

Introduction

Good quality water is essential for all living organisms[38]. However, pollutants in water are widespread, affecting nearly all water sources including lakes[2], rivers, underground water and oceans[20]. While natural phenomena such as volcanoes, storms and earthquakes can contribute to water pollution, human activities are the primary sources[1]. Among the most hazardous contaminants discharged into the environment are those from sewage treatment plants and textile industries[46].

Wastewater characteristics vary depending on the domestic and industrial sources[39]. Industries such as manufacturing, power generation, textiles, mining, nuclear and petroleum contribute significantly to wastewater production[30]. This wastewater often contains toxic and hazardous substances including heavy metals, organic toxins and solids.

Additionally, pollutants may include a broad spectrum of chemicals or pathogens[37] with many chemical substances being toxic or carcinogenic. Polluted water discharged into freshwater systems can be extremely harmful. Such contamination poses serious risks to animals and humans[40]. Even non-toxic discharges, such as oils, nutrients, or organic matter, can adversely affect the environment by depleting the oxygen levels in the water[42].

Water pollution is a significant environmental issue that affects various water sources globally. Industrial and sewage discharges are major contributors, releasing hazardous substances that pose severe health and environmental risks. Addressing this issue requires stringent measures to manage and treat wastewater effectively, ensuring the protection of water quality for all living organisms. Water pollution is a severe threat to the development of living organisms[43,47]. Among various sources, the textile industry is a major pollutant[27,28]. The industry uses water extensively in processes such as sizing, scouring, bleaching, dyeing, printing and finishing[29].

Bleaching and dyeing are particularly water-intensive[13,14]. Untreated dyes discharged from these processes can cause severe environmental damage. Both water and land are affected by the textile industry[15].

The processes within this industry require the input of a wide range of chemicals and dyestuffs, which are generally organic compounds with complex structures[31]. Water acts as the principal medium for the application of dyes and other chemicals, especially during the finishing processes[52].

Table 1
Correlation coefficient (R) and Pseudo-first-order rate constant (k) for the photo-degradation of Toludine Blue (TB) using green-synthesized TiO_2 nanoparticles

S. N.	TB concentration	Catalyst	Catalyst Volume	k min^{-1}	R	Dye Removal (%)
1	15ppm	ZnO[41]	20mg	0.2141	0.945	97.24
2	7 ppm	Mo-TiO_2[2]	140mg	76×10^{4}	—	—
3	30ppm	TiO_2 NPs*	25mg	0.763×10^{-3}	0.916	99.59

* Present work

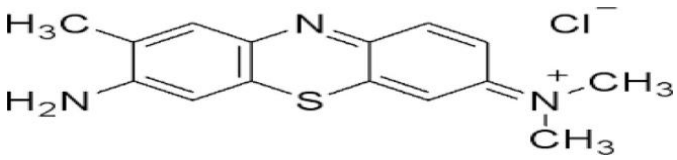

Fig. 1: Structure of Toludine Blue dye.

While the textile industry provides essential commodities, it can also have a significant environmental impact[12,18]. This pollution mainly stems from the dyeing and finishing processes[7]. If wastewater from these processes is not treated before being released back into water bodies, it can lead to decreased oxygen concentrations and reduced light penetration through the water, both of which are harmful to aquatic ecosystems[23].

Textile effluents contain numerous organic substances that are resistant to aerobic degradation and can be converted into carcinogenic agents under anaerobic conditions[6,19]. The textile industry significantly contributes to hazardous organic pollutants like dyes in water bodies. One such dye, toludine blue (TB), with the molecular formula $C_{15}H_{16}N_3SCl$, is widely used in the textile industry and poses high toxicity to humans, causing chronic effects such as anemia, weight loss and central nervous system depression.

Water purification technologies must be both cost-effective and efficient. Conventional methods like adsorption, filtration and chemical treatments are costly and can produce toxic secondary pollutants[9]. Tertiary treatments including electro-dialysis, reverse osmosis and ion exchange, are utilized. Electrolytic precipitation, which uses electric currents to precipitate and remove metal ions, requires significant contact time between the cathode and effluent[10,22]. Due to water stress, environmental contamination and resource constraints, there is growing interest in reusing wastewater from treatment facilities. Membrane bioreactors (MBRs) have gained attention for treating both municipal and industrial wastewater[21,36,49,50,53,55].

Electro-dialysis is a process that uses membranes to separate dissolved salts, driven by an electrical potential across the water, causing ions to move through a semi-permeable membrane[34]. To prevent membrane fouling, it is essential to remove suspended solids, colloids and turbidity before electro-dialysis. The ion exchange method is another common tertiary treatment, where effluents pass through beds of ion exchange resins, which can be either cationic or anionic[44]. Cationic resins remove cations from the effluent, replacing them with hydrogen ions, resulting in an acidic solution. This acidic solution, when passed through an anionic resin, has its anions substituted with hydroxyl ions[4].

TiO_2 nanoparticles (TiO_2 NPs) have various potential applications across different fields. They are used in the process of photocatalytic lead (Pb) removal from explosive industrial effluent[45]. TiO_2 nanoparticles (TiO_2 NPs) are used in biomedical applications such as cancer treatment, drug delivery, cell imaging and biosensors[26]. Additionally, novel materials like metal-organic frameworks (MOFs) and biochar-based photocatalysts have been developed to remove various refractory compounds from water in wastewater treatment[17,32].

Several studies report the synthesis of silver nanoparticles (AgNPs) and copper-silver bimetallic nanoparticles (Ag-CuNPs) using an aqueous extract of *Kigelia africana* for antimicrobial activity[5,11]. In line with green chemistry principles, fresh leaves, flowers and fruits of *Kigelia africana* (Sausage tree) are collected, dried and used to prepare extracts for synthesizing metal nanoparticles. These nanoparticles are then applied for photocatalytic degradation of organic dyes such as toludine blue (TB).

Many characterization techniques such as Scanning Electron Microscopy (SEM), Energy Dispersive X-ray Spectroscopy (EDS), Fourier-Transform Infrared Spectroscopy (FTIR), Diffuse Light Scattering (DLS), X-ray Diffraction (XRD), and Transmission Electron Microscopy (TEM) are used to investigate the stability and photocatalytic properties of the catalyst. Using Ultra-Violet-DRS facilitates the investigation of metal nanoparticle spectral properties. This method is essential for identifying possible uses for the produced nanoparticles in the environment. Furthermore, in order to investigate the photocatalytic degradation of dyes and evaluate the efficacy and efficiency of nanoparticles in

degrading organic pollutants such as dyes in wastewater, it is imperative to employ a UV-Visible Spectrophotometer.

Material and Methods

The materials and equipment used are: titanium tetra iso propoxide (Sigma-Aldrich), toludine blue (Sigma- Aldrich), hydrochloric acid (Sisco Research Lab), sodium hydroxide (Sisco Research Lab) and laboratory glassware - measuring jar (Borosil), RB-flask (Borosil), funnel (Borosil), chinna dish (Borosil) and thermometer (Borosil).

Fig. 2: Diagrammatic representations for Synthesis of TiO_2 NPs.

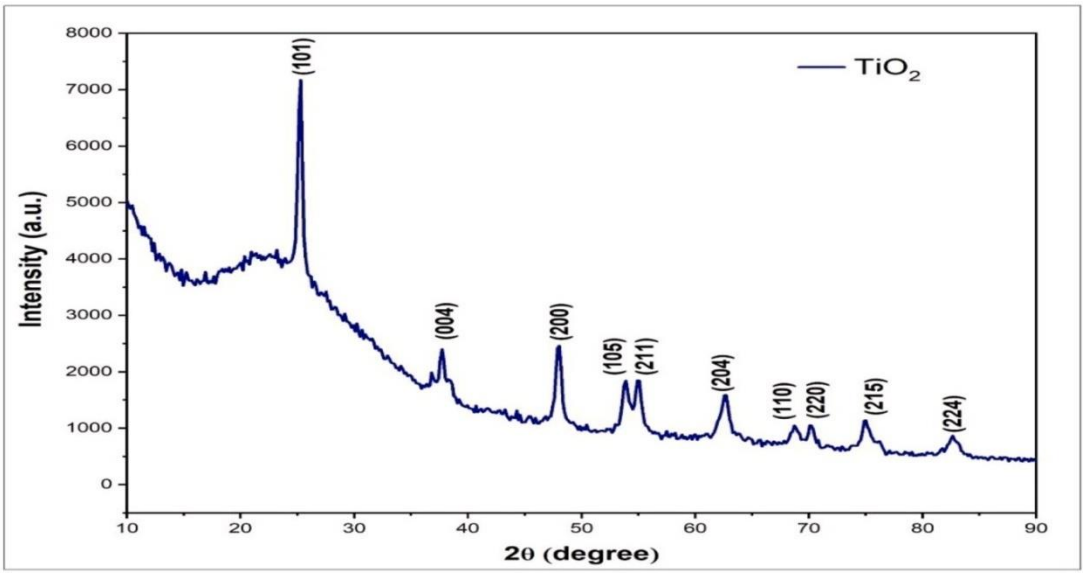

Fig. 3: Green synthesized TiO_2 NP's XRD pattern.

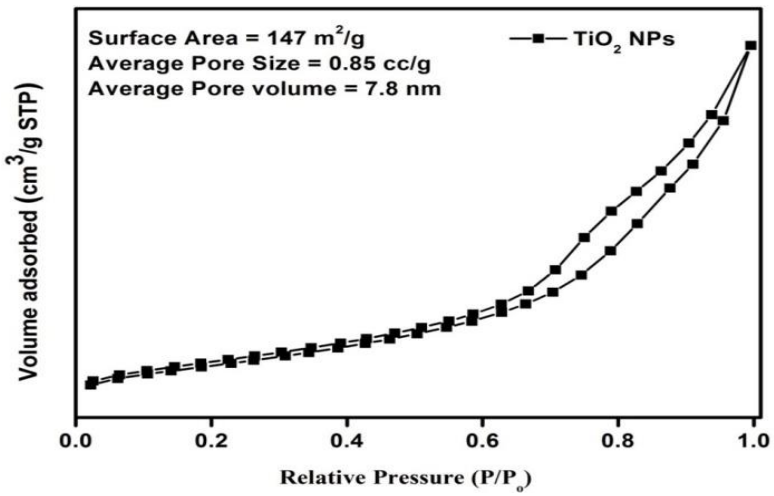

Figure 4: BET data of green synthesized TiO_2 NPs.

Plant extract preparation: Fresh *Kagelia africana* leaves were gathered and allowed to dry in the shade. After the leaves had dried, they were ground into a powder and 10 g of this powder was added to 50 ml of distilled water in a conical flask. At 50°C, the mixture was stirred for 60 minutes using a magnetic stirrer. The solution was stirred, then filtered and put to use in more experiments.

Synthesis of TiO_2 nanoparticles: 25 ml of double distilled water was combined with 5ml of leaf extract from *Kigelia africana* (sausage tree/ cucumber tree) and 5ml of titanium tetra isopropoxide (TTIP). Using a magnetic stirrer kept at 50°C for three hours, the mixture was thoroughly stirred. After that, the contents were cooled to 32°C, or at room temperature. 0.5 mm Whatmann filter paper was used to separate the white residue that had formed. After being dried for 12 hours at 100°C in an oven, the residue was calcined for 3 hours at 500°C in a Muffle furnace. After being cooled, the calcined TiO2 particles underwent characterization.

Photo-catalytic studies: Photocatalytic activity of TiO_2 nanoparticles (green synthesized) was assessed by degrading aqueous toludine blue (TB) textile dye. Initially, a stock solution of the dye at 100 ppm concentration was prepared by dissolving 10 mg of dye molecules in 100 mL of distilled water. This stock solution was further diluted to a 10 ppm working solution by mixing 1 part of the stock solution with 9 parts of distilled water.

For the catalytic experiments, 50 mL of the 10 ppm TB solution (dye concentration of 10 ppm/mL) was mixed with 50 mg of TiO_2 NPs. To ensure uniform distribution of the catalyst, the mixture was sonicated for 5 minutes. The catalytic reaction was then initiated by placing the mixture in a dark environment and allowing it to react for 1 hour under aeration to prevent catalyst settling. In the dye degradation study, 3 mL of the reaction mixture was withdrawn from the dye degradation tube at regular 5-minute intervals, centrifuged and the absorbance values were measured using a spectrophotometer. Spectral data were collected during outdoor experiments conducted from 11:30 AM to 1:30 PM, with samples taken at intervals of 0, 5, 10, 15 and 20 minutes.

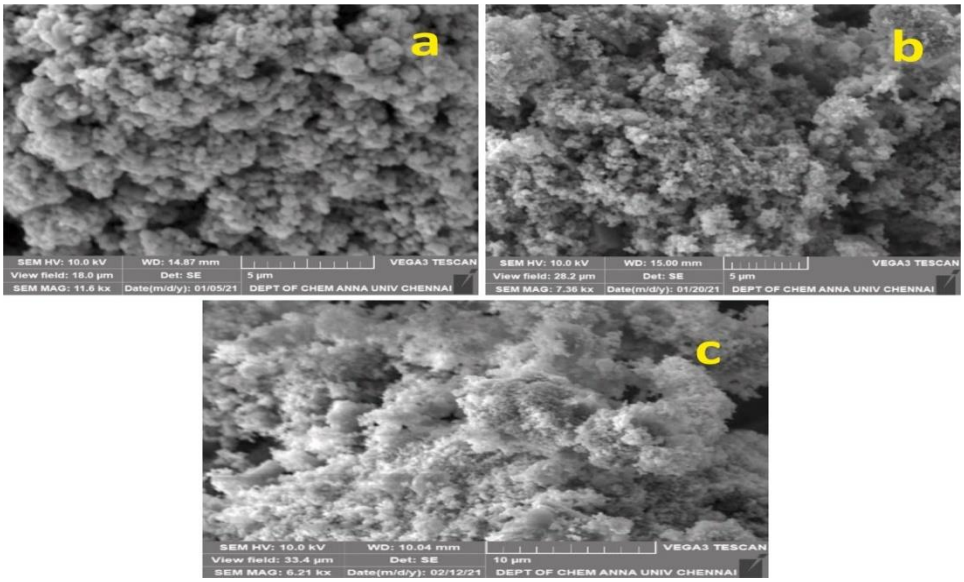

Fig. 5: SEM images of TiO_2 NPs (green synthesized) (A) Leaf extract, (B) Flower extract and (C) Fruit extract.

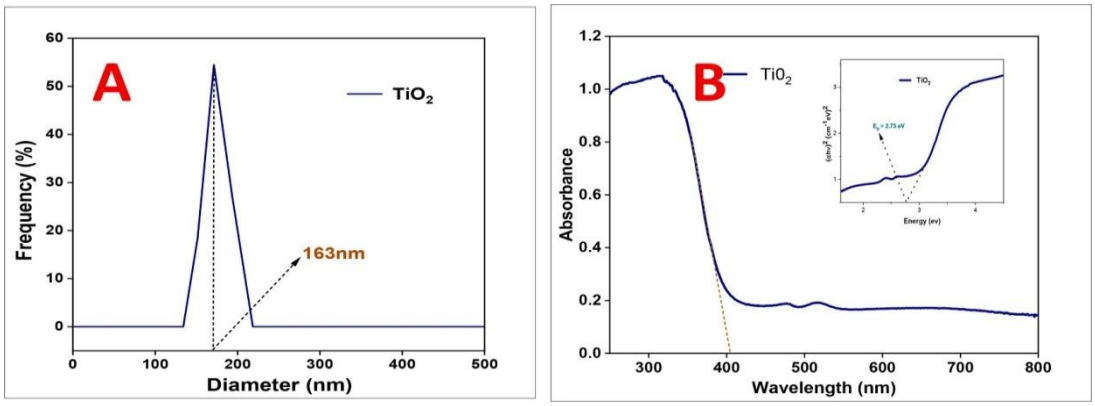

Fig. 6: (A) AFT-IR spectrum of TiO_2 NPs (green synthesized), (B) BEDAX spectrum TiO_2 NPs (green synthesized).

To assess the effect of catalyst dosage, experiments were repeated under solar exposure with different TiO_2 nanoparticle loadings (15 mg and 20 mg) while maintaining a constant dye concentration of 10 ppm. For pH optimization, dye degradation was conducted in separate 50 mL dye solutions with pH levels adjusted to 5, 7, 9 and 12.

Using green - synthesised TiO2 nanoparticles, toludine blue dye is photodegraded (Fig. 8A). The impact of changing the catalyst dosage on the TB dye degradation is shown in fig. 8B. The impact of changing dye concentration on TB dye degradation is shown in fig. 8C. With a fixed catalyst loading (50 mg for MB and 25 mg for TB), dye concentration (10 ppm/mL) and time, fig. 8D shows the impact of changing pH (adjusted using 0.1M HCl and 0.1M NaOH solutions) on TB dye degradation

Using the relevant equation, the photo-removal efficiency percentage in these experiments was determined:

Photo-removal efficiency (%) = $(C_0 - C_t) \times 100$

where C_0 is the initial concentration of the dye (in ppm) and C_t is the concentration of the dye at time t (in ppm).

This equation measures the percentage of dye removed from the solution over the course of the experiment:

% Photo-removal efficiency = $(C_0 — C_t)/C_0 * 100$

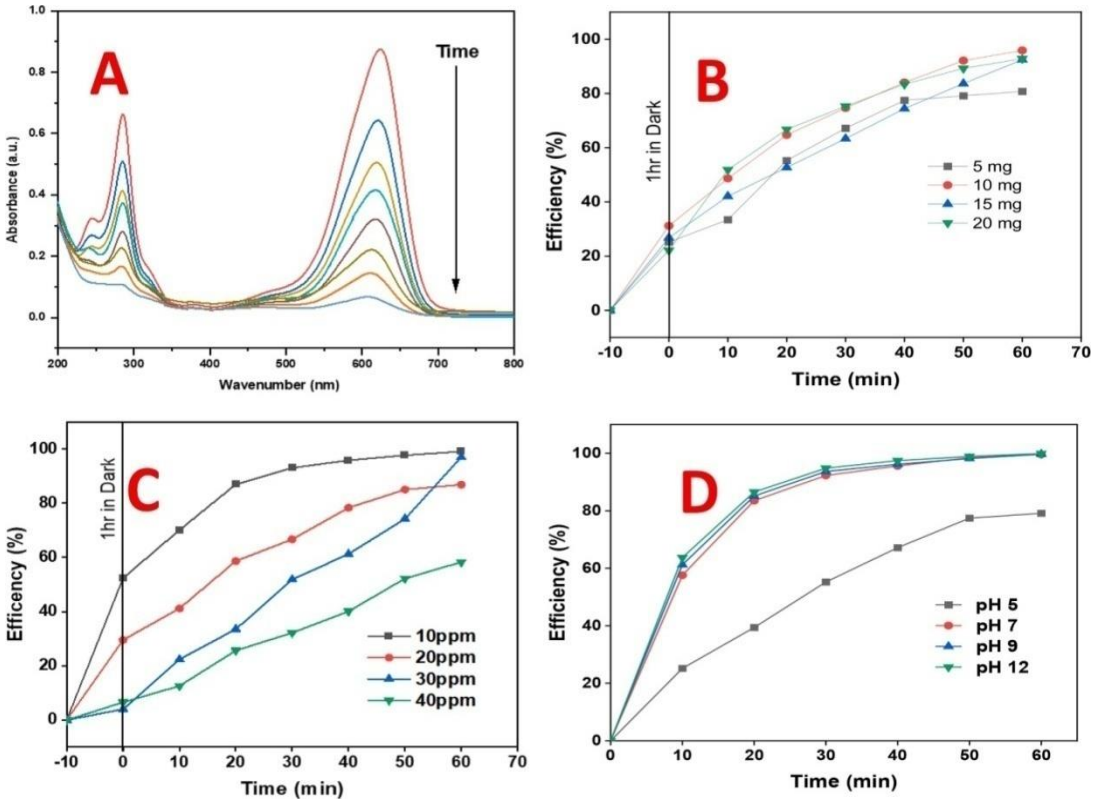

Fig. 7: ADLS plot for green synthesized TiO_2 Nanoparticle and BUV-DRS spectrum of green synthesized TiO_2 Nanoparticle.

The rate constant for the removal of dye is calculated from the following relation:

$\ln(q_e - q_t) = \ln q_e - k_1 t$

To calculate the rate constant k_1 for the degradation of toludine blue dye using green-synthesized TiO_2 nanoparticles, we typically use the pseudo-first-order kinetic model. Measure the initial concentration of toludine blue dye (C_0). Conduct the photo-degradation experiment and measure the concentration of dye at various time intervals (Ct).

Pseudo-First-Order Kinetics: The pseudo-first-order kinetic model assumes that the degradation reaction follows the rate law.

$$\ln \frac{C_0 - C_t}{C_0} \left(= -k_1 t \right)$$

where C_0 is the initial concentration of dye, C_t is the concentration of dye at time t, k_1 is the rate constant of the reaction (units: min^{-1}) and t is the time of photo-irradiation(final). q_e and q_t are amounts of dye adsorbed at equilibrium and time respectively. The rate constant k_1 is calculated from the plots of $In(q_e - q_t)$ versus time.

Higher values of k_1 is indicate faster degradation of the dye under the given experimental conditions. Ensure that the

experimental setup and conditions (such as catalyst dosage, pH and irradiation intensity) are kept consistent for accurate comparisons and calculation. This method allows to quantitatively determine the rate of dye degradation and to assess the efficiency of TiO2 nanoparticles as a photocatalyst. Quantitative analysis of the liquid products of the reactions was carried out using a Shimadzu 17A gas chromatograph (GC).

Characterization of green synthesized TiO_2: Debye-Scherrer's equation was used to determine the average crystalline size of the green-synthesised TiO_2 nanoparticles (TiO_2 NPs):

$$d = 0.89\lambda / \cos\theta$$

where θ is the Bragg's diffraction angle, β is the angular full width at half maximum, d is the average mean diameter of NPs, λ is the wavelength of the X-ray radiation source and 0.89 is a constant crystalline shape factor.

The coordination environments of TiO_2 catalysts can be analyzed by study. The diffuse reflectance spectra of the TiO_2 catalysts were performed over the range of 190–800 nm. Utilizing Perkin Elmer instruments, infrared light in the wavelength range of 4000 cm^{-1} to 670 cm^{-1} was used in the non-destructive method. FT-IR spectroscopy is non-destructive and probes molecular vibrations, providing insights into the chemical composition and bonding environments of the TiO_2 catalysts.

Utilizing a fully automated Quadra Sorbsi analyzer, Brunauer-Emmett-Teller (BET) is used to calculate material's specific surface area as a function of relative pressure through nitrogen multilayer adsorption. The experiment was carried out at liquid nitrogen temperature (-196°C) which guarantees precise surface area measurement.

Average Size was determined by using the Horiba SZ-100 Diffuse Light Scattering Instrument. Measurements were taken at a scattering angle of 90° at room temperature. Diffuse light scattering provides information on particle size distribution and average size of the synthesized nanomaterials. The integration of these methodologies yields a comprehensive understanding of the structural, electronic and surface characteristics of TiO_2 catalysts, which is essential for comprehending their efficacy and potential uses in diverse catalytic procedures.

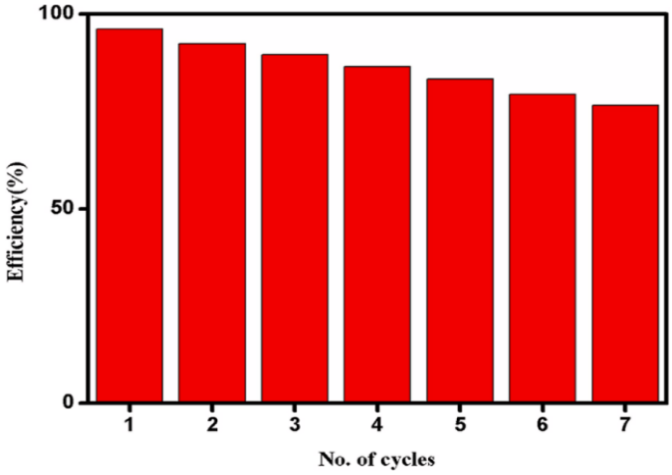

Fig. 8: Recycling efficacy chart of green synthesized catalyst.

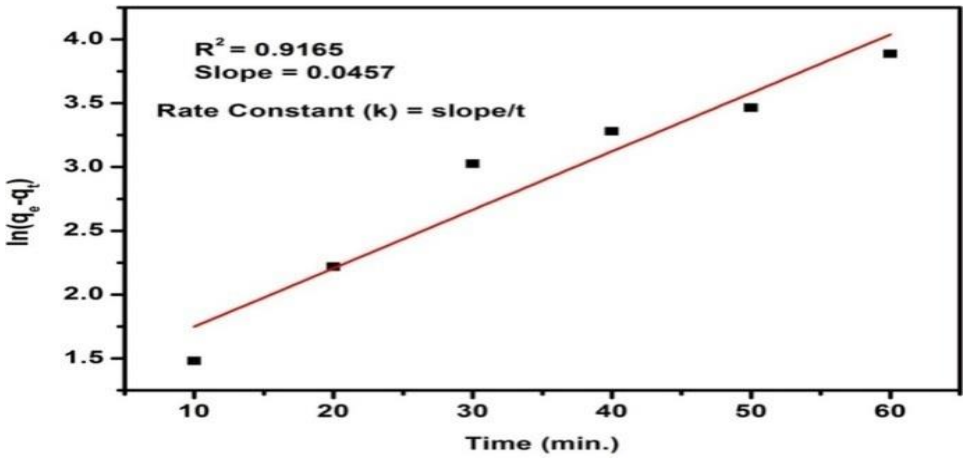

Fig. 9: Pseudo-first order kinetics model of TB dye Photodegradation of XRD peaks recorded at 2θ Shimadzu UV-1800 DRS UV–Visible spectrophotometer.

Results and Discussion

Characteristics of green synthesized TiO_2

XRD pattern: The X-Ray diffraction pattern of TiO_2 nanoparticles (Green synthesized) in fig. 3 confirms their crystalline nature, highlighting the presence of the anatase phase. This phase characterization is essential for assessing the nanoparticles' crystallinity, crystal structure and phase purity, which are key factors influencing their properties and applications in fields such as photocatalysis and sensing.

The XRD pattern of the green synthesized TiO2 NPs (Fig. 3) showed various peaks in a wide range of 2θ angle (10 <2θ <80), revealing that the distinct peaks recorded at 25.37◦, 37.72◦, 48.04◦, 53.82◦, 55.07◦, 62.71◦, 68.76◦, 70.27◦ and 74.84◦ well corresponded to the Miller indices values, (101), (004), (200), (105), (211), (204), (110), (220) and (215) respectively confirming the anatase phase (JCPDS 21–1272)[48]. The average crystalline TiO2 NPs were measured using XRD peaks using Debye Scherrer's equation and the value is 17.5 nm. The crystallite size is less compared to the commercial TiO2 P25 (20.97nm). Hence, it is clear that the green synthesized method is beneficial for producing the TiO_2 NPs with reduced size[8].

SEM images: SEM analysis of the green-synthesized TiO_2 nanoparticles (TiO_2 NPs), as shown in fig. 5, revealed spherical particles with diameters ranging from 50 to 200 nm. The images clearly depicted numerous small, well-defined TiO_2 NPs alongside a smaller number of larger agglomerated NPs. The agglomeration observed could be attributed to the low pH of the TiO_2 NP solution.

However, the presence of phytochemicals such as polyphenols, flavonoids, alkaloids, antioxidants, terpenoids, steroids, free amino acids and tannins from the leaves of the Sausage tree acted as capping agents. These compounds played a crucial role in enhancing NP dispersion and reducing agglomeration during synthesis. This capability is beneficial for producing various types of nanoparticles with improved dispersion characteristics, potentially enhancing their applications in different fields.

FT-IR spectrum: The FT-IR spectrum of the green synthesized TiO2 NPs recorded in the series of absorption bands 500cm^{-1} to 4000cm^{-1} is shown in fig. 6A. The band intensities in the different regions of the spectrum recorded for the powdered TiO2 NPs were analyzed. Abroad peak at 3228cm^{-1} and a small peak at 1631cm^{-1} was possibly attributed to the presence of the hydroxy l group and surface-adsorbed water respectively[16]. The hydroxyl group might be contributed to the enhancement of photocatalytic activity. When the amount of hydroxyl group increased on the surface of TiO_2 NPs, the OH largely increased, this is responsible for the higher electron transportability and thus, enhanced the photocatalytic activity.

An absorption peak at 500–900cm^{-1} may correspond to Ti–O stretching and Ti–O–Ti bridging stretching modes24. As reported earlier, the absorption peak at 799cm^{-1} possibly indicated the contribution of the anatase phase of the green synthesized TiO2 NPs. However, no peak was recorded at 2900cm for the C– H stretching band that ensured the removal of all the organic compounds from the sample during the calcination process.

EDAX pattern: TiO_2 nanoparticles synthesized using green methods had their elemental composition determined using an X-ray Energy Dispersive Spectrometer (ESD). The presence of titanium (Ti) and oxygen (O) as the main elements is confirmed by the EDX spectrum displayed in fig. 6B which also shows the sample's purity. Ti and O have weight percentages of 81.32% and 18.68% respectively and atomic percentages of 59.26% and 40.74% respectively. Since the elemental composition of the nanoparticles matches the expected composition of TiO_2, this analysis offers compelling evidence in favor of the green synthesis of TiO^2 nanoparticles. The successful formation of TiO_2 nanoparticles via the green synthesis route is further confirmed by the presence of these elements in the specified ratios.

DLS plot: The particle size distribution of the green synthetic TiO_2 nanoparticles was ascertained using the dynamic light scattering (DLS) technique. In order to prepare the representative solution that was used to ascertain the particle size distribution, the powdered TiO_2 NPs were first thoroughly dissolved in distilled water. This was followed by ultra-sonication to achieve the uniform distribution of NPs. Further proof of the environmentally friendly synthesis of nanosized TiO_2 was provided by the DLS plot displayed in figure 7A which showed that a maximum intensity was achieved at an average particle size of 163 nm. This provided additional support for the SEM study's determination of the green synthesized TiO_2 NPs' particle size range.

UV-DRS spectrum: The absorption spectrum of TiO_2 nanoparticles (green-synthesized), as depicted in figure 7B, exhibits a prominent absorption peak at 405 nm within the wavelength range of 200 to 800 nm. This absorption peak is characteristic of TiO_2 nanoparticles and provides clear evidence of their green synthesis.

Additionally, the Tauc plot shown in Fig. 7B illustrates the relationship between photon energy (hνh\nuhν) and the quantity (αhν\alphah\nuαhν)^2 on the Y-axis. By extrapolating the linear portion of the curve to the X-axis, the direct band gap energy of the green-synthesized TiO_2 NPs was determined to be 3.68 eV. This value indicates strong quantum confinement effects in the TiO_2 nanoparticles, likely due to their nanoscale dimensions and specific synthesis method.

Overall, these optical analyses confirm the successful green synthesis of TiO_2 NPs and provide insights into their band gap energy, which is crucial for understanding their optical

properties and potential applications in photocatalysis, sensing and other advanced technologies.

Photo catalytic activities: The photo catalytic activities of the green synthesized TiO_2 NPs have been studied under solar light using Toludine blue (TB) dye as a substrate fig. 8. The photo-degradation of Toludine blue dye on synthesized TiO_2 NPs is shown in fig. 7A.

Effect of catalyst dosage: Increasing TiO_2 nanoparticle (TiO_2 NPs) dosage enhances photocatalytic efficiency for toludine blue (TB) dye degradation under solar light by providing more active sites and surface area for reactions (Fig. 8B). Efficiency improves from 82.99% to 98.19% as dosage increases from 5 mg to 20 mg due to increased active species concentration. However, efficiency may plateau or slightly decrease beyond 20 mg due to reduced light penetration and particle aggregation. Optimizing TiO_2 NP dosage, along with dye concentration, pH and irradiation time, is crucial for maintaining high and consistent degradation efficiency in photocatalysis.

Effect of dye concentration: In fig. 8C, increasing toluidine blue (TB) dye concentration diminishes the availability of reactive species like OH radicals on the catalyst surface due to heightened competition for light absorption with TiO_2 nanoparticles (TiO_2 NPs). This reduces photon penetration to TiO_2 NPs, thereby limiting efficient degradation. Consequently, higher dye concentrations result in slower degradation rates and reduced overall efficiency, high lighting the importance of balancing dye concentration, TiO_2 NP dosage and light exposure for optimizing photo-catalytic performance under solar irradiation.

Effect of pH: In fig. 8D, TB dye interaction with the catalyst surface across pH 5 to 12 reveals enhanced efficiency at basic pH levels due to strong electrostatic interactions with the catalyst. Efficiency decreases gradually as pH decreases from 12 to 5, with no degradation observed at pH 3. Specific efficiencies include 80.92% at pH 5, 99.52% at neutral pH 7 and 99.89% at pH 9 and 12, indicating optimal degradation conditions. Mechanistically, lower pH values hinder efficiency due to electrostatic repulsion between positively charged TB dye molecules and the negatively charged catalyst surface, while higher pH enhances attraction and facilitates effective adsorption and degradation. Optimizing pH is critical for maximizing TiO_2 nanoparticle-based photocatalytic efficiency in TB dye degradation, emphasizing the need for maintaining a basic pH environment for optimal performance.

Photo-catalytic activity: Materials with porous structures and large specific surface areas are known to significantly enhance photocatalytic activity by providing ample reactive sites for efficient adsorption and interaction with organic contaminants. These characteristics also reduce mass transfer resistance, facilitating rapid diffusion of reactants and products. Furthermore, the shortened migration distance of photo generated charge carriers within these materials further boosts their efficiency in photocatalytic processes. Recent studies[33,51,54] highlight the pivotal role of these textural properties in optimizing photocatalytic performance across diverse applications.

Green-synthesized TiO_2 has been shown to effectively capture excited electrons and transfer them to surface-adsorbed oxygen molecules, preventing electron-hole recombination and facilitating the generation of superoxide radicals. These radicals play a crucial role in transforming pollutant molecules into less harmful compounds during toluidine blue (TB) dye photodegradation. The pseudo first-order kinetics observed from ln(qe-qt) vs. time(t) plots indicated a linear relationship, confirming efficient TB degradation by TiO_2 NPs. The computed apparent rate constant (k) of 0.000763 min^{-1} underscores the photocatalytic efficacy of the synthesized nanoparticles (Table 1).

Reusability studies: The green-synthesized catalyst underwent centrifugation, washing and activation for multiple cycles, revealing a gradual decline in photocatalytic efficiency over 7 cycles (Fig. 9). This decrease can be attributed to the accumulation of reaction by-products and possibly the blocking of active sites on the catalyst surface. Despite the slight decline in performance with reuse, the catalyst demonstrates potential for multiple cycles of photocatalytic activity.

Our findings indicate that the decrease in efficiency observed with each cycle of the spent catalyst could be attributed to material loss during the recovery process. Despite this, the catalyst demonstrates stability and maintains its efficiency up to the 7th cycle, suggesting its suitability for repeated use without significant loss in effectiveness. This reusability enhances its efficiency and economic viability, underscoring its potential for various industrial applications.

Conclusion

Using a green synthesis approach with extracts from the Sausage tree, TiO_2 NPs were successfully synthesized in this study with high yields and were characterized for their desirable textural properties and morphology. Optimal conditions for dye degradation were determined as pH 7, 30 ppm TB dye concentration and a catalyst dosage of 10 mg in 50 mL. The TiO_2 NPs efficiently degraded the dye within 60 minutes, following a pseudo-first-order kinetics model as previously described. This reusability factor enhances the efficiency and economic feasibility of the synthesized TiO_2 catalyst.

References

1. Agyare C., Dwobeng A.S., Agyepong N., Boakye Y.D., Mensah K.B., Ayande P.G. and Adarkwa-Yiadom M., Antimicrobial, antioxidant and wound healing properties of Kigelia africana (Lam.) Beneth. and Strophanthus hispidus DC., *Adv. Pharmacol.*

Sci., https://doi.org/10.1155/2013/692613 **(2013)**

2. Amanulla A.M. and Sundaram R.J.M.T.P., Green synthesis of TiO2 nanoparticles using orange peel extract for antibacterial, cytotoxicity and humidity sensor applications, *Mater. Today: Proc*., **8**, 323–331 **(2019)**

3. Ameta R., Sharma S., Sharma S. and Gorana Y., Visible light induced photocatalytic degradation of toluidine blue-O by using molybdenum doped titanium dioxide, *Eur. J. Adv. Eng. Technol*. **2(8)**, 95–99 **(2015)**

4. Anantharaman A., Ramalakshmi S. and George M., Green synthesis of calcium oxide nanoparticles and its applications, *Int. J. Eng. Res. Afr*., **6(10)**, 27e31 **(2016)**

5. Ashishie P.B., Anyama C.A., Ayi A.A., Oseghale C.O., Adesuji E.T. and Labulo A.H., Green synthesis of silver monometallic and copper-silver bimetallic nano particles using Kigelia africana fruit extract and evaluation of the iranti microbial activities, *Int. J. Phys. Sci*., **13(3)**, 24–32 **(2018)**

6. Bharagava Chandra R.N., Yadav S. and Mohan D., Accumulation and distribution of toxic metals in wheat (Triticum aestivum L.) and Indian mustard (Brassicacampestris L.) irrigated with distillery and tannery effluents, *J. Hazard Mater*., **162**, 1514–1521 **(2009)**

7. Dette M.A. P´erezOsorio, Kley C.S., Punke P., Patrick C.E., Jacobson P., Giustino F., Jung S.J. and Kern K., TiO_2 Anatase with a band gap in the visible region, *Nano Lett*., **14**, 6533–6538 **(2014)**

8. Gonza´lez-Burciaga L.A., Nún˜ez-Nún˜ez C.M., Morones-Esquivel M.M., Avila-Santos M., Lemus-Santana A. and Proal-N´ajera J.B., Characterization and comparative performance of TiO2 photocatalysts on 6-mercaptopurine degradation by solar heterogeneous photo catalysis, *Catalysts*, **10(1)**, 118 **(2020)**

9. Jayamohan Harikrishnan, Smith York R., Gale Bruce K., Mohanty Swomitra K. and Misra Manoranjan, Photocatalytic micro fluidic reactors utilizing titania nanotubes on titanium mesh for degradation of organic and biological contaminants, *J. Environ. Chem. Eng*., **4(1)**, 657–663 **(2016)**

10. Joshi K.M. and Shrivastava V.S., Photocatalytic degradation of Chromium (VI) from wastewater using nanomaterials like TiO_2, ZnO and CdS, *Appl. Nanosci*., **1(3)**, 147–155 **(2011)**

11. Kalainila P., Ravindran R.E., Rohit R. and Renganathan S., Anti-bacterial effect of bio-synthesized silver nanoparticles using *Kigelia Africana*, *J. Nanosci. Nanoeng*., **1**, 225–232 **(2015)**

12. Karakitsou X.E. Verykios, Effects of altervalent cation doping of TiO_2 on its performance as a photocatalyst for water cleavage, *J. Phys. Chem.*, **97**, 1184–1189 **(1993)**

13. Khade M.B. Suwarnkar, Gavade N.L. and Garadkar K.M., Green synthesis of TiO2 and its photo catalytic activity, *J. Mater. Sci*., **26**, 3309–3315 **(2015)**

14. Khandayataray P., Murthy M.K., Samal D. and Gurusubramanian G., Sustainable Integrated Pest Management using Pheromones: Types, Synthesis, Mechanism of Action and Applications, *Res. J. Biotech.*, **19(2)**, 140-157 **(2024)**

15. Li W., Du D., Yan T., Kong D., You J. and Li D., Relationship between surface hydroxyl groups and liquid-phasephotocatalytic activity of titanium dioxide, *J. Colloid Interface Sci*., **444**, 42–48 **(2015)**

16. Liu Shouxin and Chen Xiaoyun, Preparation and characterization of a novel activated carbon-supported N-doped visible light response photo catalyst (TiO_2—xNy/AC), *J. Chem. Technol. Biotechnol.: Int. Res. Process Environ. Clean Technol*., **82(5)**, 453–459 **(2007)**

17. Liu X., Verma G., Chen Z., Hu B., Huang Q., Yang H. and Wang X., Metal- organic framework nanocrystals derived hollow porous materials: syntheticstrategies and emerging applications, *The Innovation*, Doi: 10.1016/j.xinn.2022.100281, 100281 **(2022)**

18. Lopez R. Gomez, Band-gap energy estimation from diffuse reflectance measurements on sol-gel and commercial TiO_2: a comparative study, *J. Sol-Gel Sci.Technol*., **61**, 1–7 **(2012)**

19. Malakutian Mansuri F., Hexavalent chromium removal by titanium dioxide photocatalytic reduction and the effect of phenol and humicacidonits removal efficiency, *Int. J. Environ. Health Eng*., **4**, 1–8 **(2015)**

20. Manjunatha K.G., Swamy B.K., Madhuchandra H.D. and Vishnumurthy K.A., Synthesis, characterization and electrochemical studies of titanium oxide nanoparticle modified carbon paste electrode for the determination of paracetamolin presence of adrenaline, *Chem. Data Collect*., **31**, 100604 **(2021)**

21. Meng Shujuan et al, The role of transparent exopolymer particles (TEP) in membrane fouling: a critical review, *Water Res*., **181**, 115930 **(2020)**

22. Mishra Sandhya and Bharagava Ram Naresh, Toxic and genotoxic effects of hexavalent chromium in environment and its bioremediation strategies, *J. Environ.Sci. Health Part C*, **34(1)**, 1–32 **(2016)**

23. Moniema M.E.M. Ali, Gad-Allaha T.A., Khalil A.S.G., Ulbricht M., El-Shahat M.F., Ashmawy M.A. and Ibrahima H.S., Detoxification of hexavalent chromium in waste water containing organic substances using simonkolleite-TiO_2 photocatalyst, *Process Saf. Environ. Prot*., **95**, 247–254 **(2015)**

24. Myilsamy M., Mahalakshmi M., Murugesan V. and Subha N.J.A.S.S., Enhanced photocatalytic activity of nitrogen and indium co-doped mesoporous TiO_2 nanocomposites for the degradation of 2, 4-dinitrophenol under visible light, *Appl. Surf. Sci*., **342**, 1–10 **(2015a)**

25. Myilsamy M., Murugesan V. and Mahalakshmi M., Indium and cerium co-doped mesoporous TiO_2 nanocomposites with enhanced visible light photocatalytic activity, *Appl. Catal. A*, **492**, 212–222 **(2015b)**

26. Nabi Ghulam, Khalid N.R., Bilal Tahir M., Rafique Muhammad, Rizwan Muhammad, Hussain Sajad, Iqbal Tahir and Majid Abdul, A review on novel eco-friendly green approach to synthesis TiO_2 nanoparticles using different extracts, *J. Inorg. Organomet. Polym. Mater*., **28(4)**, 1552–1564 **(2018)**

27. Neelakandeswari N. et al, Spectroscopic investigations on the

photodegradation of toluidine blue dye using cadmium sulphide nanoparticles prepared by a novel method, *Spectrochim. Acta Mol. Biomol. Spectrosc*., **78(5)**, 1592e1598 **(2011)**

28. Nguyen C.H., Fu C.C. and Juang R.S., Degradation of methylene blue and methyl orange by palladium-doped TiO_2 photocatalysis for water reuse: efficiency and degradation pathways, *J. Clean. Prod.*, **202**, 413e427 **(2018)**

29. Niju S., Meera K.M., Begum S. and Anantharaman N., Modification of egg shell and its application in biodiesel production, *J. Saudi Chem. Soc*., **18(5)**, 702e706 **(2014)**

30. Nithya M. et al, Green synthesis of A-Fe2O3/bipo4 composite and its biopolymeric beads for enhanced photocatalytic application, *J. Mater. Sci. Mater. Electron*., **29**, 14733e14745 **(2018)**

31. Peiro J. Peral, Domingo C., Momenech X. and Ayllon J.A., Low-temperature deposition of TiO_2 thin films with photocatalytic activity from colloidal anatase aqueous solutions, *Chem. Mater*., **13**, 2567–2573 **(2011)**

32. Qiu M., Liu L., Ling Q., Cai Y., Yu S., Wang S. and Wang X., Biochar for the removal of contaminants from soil and water: a review, *Biochar*, **4(1)**, 1–25 **(2022)**

33. Qiu Muqing, Hu Baowei, Chen Zhongshan, Yang Hui, Zhuang Li and Wang Xiangke, Challenges of organic pollutant photocatalysis by biochar-based catalysts, *Biochar*, **3(2)**, 117–123 **(2021)**

34. Qu P.J.J. Alvarez and Li Q., Applications of nanotechnology in water and waste water treatment, *Water Res*., **47**, 3931–3946 **(2013)**

35. Ramya R., Krishnan P.S., Neelaveni M., Gurulakshmi M., Sivakumar T. and Shanthi K., Enhanced visible light activity of Pr–TiO_2 nanocatalyst in the degradation ofdyes: effect of Pr doping and TiO_2 morphology, *J. Nanosci. Nanotechnol*., **19(7)**, 3971–3981 **(2019)**

36. Riccardo Campo, Lubello Claudio, Lotti Tommaso and Bella Gaetano Di, Membrane fouling in aerobic granulars ludge (AGS)-membrane bioreactor (MBR): effect of AGS size, *Water Res.*, **157**, 445–453 **(2019)**

37. Rossetto E., Petkowicz D.I., dos Santos J.H., Pergher S.B. and Penha F.G., Bentonites impregnated with TiO2 for photodegradation of methylene blue, *Appl. Clay Sci*., **48(4)**, 602e606 **(2010)**

38. Roy A., Bulut O., Some S., Mandal A.K. and Yilmaz M.D., Green synthesis of silver nanoparticles: biomolecule-nanoparticle organizations targeting antimicrobial activity, *RSC Adv.*, **9(5)**, 2673–2702 **(2019)**

39. Saeed M., Usman M. and ul Haq A., Catalytic degradation of organic dyes in aqueous medium, *Photochem. Photophys. Fundam. Appl.*, DOI: 10.5772/intechopen.75008,197 **(2018)**

40. Safaei-Ghomi J., Ghasemzadeh M.A. and Mehrabi M., Calcium oxide nanoparticles catalyzed one-step multi component synthesis of highly substituted pyridines in aqueous ethanol media, *Sci. Iran*, **20(3)**, 549e554 **(2013)**

41. Salim H.A.M., Idrees S.A., Rashid R.A., Mohammed A.A., Simo S.M. and Khalo I.S., Photo-catalytic degradation of toludine blue dye in aqueous medium under fluorescent light, In 2018 International Conference on Advanced Science and Engineering (ICOASE), *IEEE*, 384–388 **(2018)**

42. Samsudin M.F.R., Sufian S., Bashiri R., Mohamed N.M., Siang L.T. and Ramli R.M., Optimization of photodegradation of methylene blue over modified TiO2/BiVO4 photocatalysts: effects of total TiO2 loading and different type of co-catalyst, *Mater. Today: Proc*., **5(10)**, 21710e21717 **(2018)**

43. Sawant S.A., Somani S.P., Omanwar S.K. and Somani P.R., Chemical and photocatalytic degradation of crystal violet dye by Indian edible chuna (calcium oxide/hydroxide), *J Green Sci. Technol*., **2(1)**, 45e48 **(2015)**

44. Saxena R. Chandra and Bharagava R.N.., Environmental pollution, toxicity profile and treatment approaches for tannery waste water and its chemical pollutants, *Rev. Environ. Contam. Toxicol*., **240**, 31–69 **(2016)**

45. Sethy Naresh Kumar et al, Green synthesis of TiO_2 nanoparticles from Syzygium cumini extract for photo-catalytic removal of lead (Pb) in explosive industrial wastewater, *Green Process. Synth*., **9(1)**, 171–181 **(2020)**

46. Singh A. and Sheikh J., Cleaner functional dyeing of wool using Kigelia Africana natural dye and Terminalia chebula bio-mordant, *Sustain. Chem. Pharm*., **17**, 100286 **(2020)**

47. Tangboriboon N., Kunanuruksapong R. and Sirivat A., Preparation and properties of calcium oxide from egg shells via calcination, *Adv. Mater. Sci.* (Warsaw, Poland), **30(4)**, 313e322 **(2012)**

48. Wang Qizhao, Lian Juhong, Bai Yan, Hui Juan, Zhong Junbo, Li Jianzhang, An Ning, Yu Jie and Wang Fangping, Photocatalytic activity of hydrogen production from water over TiO_2 with different crystal structures, *Mater. Sci. Semicond. Process.*, **40**, 418–423 **(2015)**

49. Wensong Chen, Mo Jiahao, Du Xing, Zhang Zhien and Zhang Wenxiang, Biomimetic dynamic membrane for aquatic dye removal, *Water Res.*, **151**, 243–251 **(2019)**

50. Wenxiang Zhang, Liang Wenzhong, Zhang Zhien and Hao Tianwei, Aerobic Granular Sludge (AGS) scouring to mitigate membrane fouling: performance, hydrodynamic mechanism and contribution quantification model, *Water Res.*, **188**, 116518 **(2021)**

51. Yao Ling, Yang Hui, Chen Zhongshan, Qiu Muqing, Hu Baowei and Wang Xiangxue, Bismuth oxychloride-based materials for the removal of organic pollutants in wastewater, *Chemosphere*, **273**, 128576 **(2021)**

52. Yu J., Su Y., Cheng B. and Zhou M., Effects of pH on the microstructures and photocatalytic activity of mesoporous nano-crystalline titania powders prepared via hydrothermal method, *J. Mol. Catalysis A: Chem*., **258**, 104–112 **(2006)**

53. Zhang Sai et al, Molybdenum (VI)-oxo clusters incorporation

activates g-C3N4 with simultaneously regulating charge transfer and reaction centers for boosting photocatalytic performance, *Adv. Funct. Mater*., **32(38)**, 2204175 **(2022a)**

54. Zhang Y., Liu H., Gao F., Tan X., Cai Y., Hu B. and Wang X., Application of MOFs and COFs for photocatalysis in CO_2 reduction, H_2 generation and environmental treatment, *Energy Chem*, **4**, 100078 **(2022b)**

55. Zhenzhou Zhu, Chen Zhe, Luo Xiao, Zhang Wenxiang and Meng Shujuan, Gravity-driven biomimetic membrane (GDBM): an ecological water treatment technology for water purification in the open natural water system, *Chem. Eng. J*., **399**,125650 **(2020)**.

(Received 05th August 2024, accepted 18th September 2024)